

# Learning Representations by Humans, for Humans

Sophie Hilgard<sup>\*1</sup>, Nir Rosenfeld<sup>\*2</sup>, Mahzarin Banaji<sup>3</sup>, Jack Cao<sup>3</sup>, David C. Parkes<sup>1</sup>

<sup>1</sup> School of Engineering and Applied Science, Harvard University

<sup>2</sup> Computer Science Department, Technion - Israel Institute of Technology

<sup>3</sup> Department of Psychology, Harvard University

## Abstract

The task of optimizing machines to support human decision-making is often conflated with that of optimizing machines for accuracy even though they are materially different. Whereas it is typical for learning systems to prescribe actions through prediction, here we propose an approach in which the role of machines is to reframe problems in order to directly support human decisions. Inspired by the success of representation learning in promoting machine performance, we frame the problem as one of learning representations that are conducive to good human performance. This “Man Composed with Machine” framework incorporates a human decision-making model directly into the representation learning paradigm with optimization achieved through a novel human-in-the-loop training procedure. We empirically demonstrate the successful application of the framework to various tasks and representational forms.

## 1 Introduction

*“No one ever made a decision because of a number.  
They need a story.”*

— Daniel Kahneman

Advancements in machine learning algorithms, as well as increased data availability and computational power, have led to the rise of predictive machines that outperform human experts in controlled experiments (Esteva et al. 2017; Nickerson and Rogers 2014). And yet, there is broad recognition that human involvement remains important (Liu et al. 2019), especially in domains in which safety and equity are important considerations (Parikh, Obermeyer, and Navathe 2019; Barabas et al. 2017), and with users have external information or want to exercise agency and use their own judgment.

At the same time, as humans we are limited in our capacity to make good decisions. We are bound by our cognitive capabilities and prone to psychological biases (related to, e.g., framing and heuristics), which make it difficult to identify and rightly act upon complex patterns emerging in data (Kahneman 2011; Miller 1956). Given that pattern recognition is the hallmark of machine learning, there is a clear opportunity for data-driven, human-computer collaboration.

Work in facilitating human-machine collaboration has focused on *interpretable machine learning*, which augments

machine predictions with explanations about a prediction (Ribeiro, Singh, and Guestrin 2016; Lakkaraju et al. 2019; Lundberg and Lee 2017). Important as it is, we see two main drawbacks to this approach. First, setting the role of machines to predict and then explain serves to reduce humans to auditors of the ‘expert’ machines (Lai and Tan 2018). With loss of agency, people are reluctant to adopt predictions and even inclined to go against them (Bandura 1989, 2010; Yeomans et al. 2017; Dietvorst, Simmons, and Massey 2016; Yin, Vaughan, and Wallach 2019; Green and Chen 2019b). This leads to a degradation in performance of the human-machine pipeline over time (Elmalech et al. 2015; Dietvorst, Simmons, and Massey 2015; Logg 2017; Stevenson and Doleac 2018). Second, these methods cannot adapt to the way in which predictions are used, are unable to adjust for systematic human errors or inconsistencies, and fail to make use of human capabilities.

Here we introduce the ‘Man Composed with Machine’ framework (M◊M), aiming to bridge the paradigm of machine learning with that of human-centric design (Sutton et al. 2020; Venkatesh et al. 2003), and advocate for a broader perspective on using machine learning in support of decision-making. We make two key contributions. First, rather than machines that predict or decide, we train models that learn how to *reframe problems* for a human decision-maker. We learn to map problem instances to representational objects such as plots, summaries, or avatars, aiming to capture problem structure and maintain user autonomy. This approach of “advising through reframing” draws on a large body of work in the social sciences that shows that the quality of human decisions depends on how problems are presented (Thompson 1980; Cosmides and Tooby 1992; Gigerenzer and Hoffrage 1995; Kahneman and Tversky 2013; Brown et al. 2013). Second, rather than optimizing for machine performance, we *directly optimize for human performance*. We learn representations of inputs for which human decision-makers perform well rather than those under which machines achieve high accuracy.

We use a human-in-the-loop procedure for training end-to-end both the machine model and a proxy model of human decision making, where human decisions given the current representation are used to update the representation and improve decisions. We demonstrate the framework on three distinct tasks, each highlighting a different aspect of our

<sup>\*</sup>Equal contribution, alphabetical order.

approach and exploring different forms of representations. We first use the controlled environment of *point clouds* to show how the framework can learn scatter-plot representations that allow for high human accuracy without explicitly presenting a recommended action. The second experiment is in the setting of loan approvals, and adopts *facial avatars* as representational advice—with the goal of exploring what representations are learned and how they are used to support decision-making. Our third experiment is simulative and designed to demonstrate the novel capacity of our framework to learn how to best enable the incorporation of *side-information*—even while this is known only to the user—and achieve better performance than either human or machine alone. Collectively, these experiments showcase this new approach to machine learning as a tool for human-intelligence augmentation (Licklider 1960; Engelbart 1962).

**On the use of facial avatars:** In our study on loan approval we convey advice through a facial avatar representing an algorithmic assistant. We experiment with facial avatars as representations because they are high dimensional, abstract (relative to the domain studied), and accessible to people. Any use of facial representations in consequential decision settings must be done with care, and we are aware of the legitimate concerns regarding the use of faces in AI systems, especially in regard to discrimination (West and Crawford 2019). We take care to minimize these concerns, ensuring that users understand that the avatar represents an algorithmic assistant and not a loan applicant, and restricting to carefully chosen variations on the image of the single actor.

## 1.1 Additional Related Work

**Modeling human factors and machine arbiters.** Recent studies have shown that the connections between trust, accuracy, and explainability can be complex and nuanced (Green and Chen 2019a; Lai and Tan 2018). For example, users fail to consistently increase trust in a model even when model accuracy is superior to human accuracy and models are modified to make them more interpretable (Yin, Vaughan, and Wallach 2019; Poursabzi-Sangdeh et al. 2018). At the same time, there is a tension, in that whether or not users retain agency has been shown to affect acceptance of model predictions (Dietvorst, Simmons, and Massey 2016), providing support for the approach we take with MoM. Other work considers learning when to predict, in effect bypassing human arbitration, and when to defer to the user (Madras, Pitassi, and Zemel 2018). Recent work acknowledges that human decision processes must be considered when developing decision support technology (Lai, Carton, and Tan 2020; Bansal et al. 2019), and work in cognitive science has shown settings in which accurate models of human decision-making can be developed (Bourgin et al. 2019).

**Model interpretability for human arbiters.** Much of the interpretability literature also follows our paradigm of humans as the final decision-makers, with interpretable models enabling users to bring to bear additional criteria (e.g., fairness) that can be difficult to automate (Doshi-Velez and Kim 2017); e.g., by simplifying inputs (Angelino et al. 2017; Lakkaraju, Bach, and Leskovec 2016) or augmenting in-

puts (Ribeiro, Singh, and Guestrin 2016; Smilkov et al. 2017; Lei, Barzilay, and Jaakkola 2016) in order to help users understand the way data is being used. This work generally optimizes interpretability proxies (Lage et al. 2019) in combination with machine accuracy, using humans only to validate at test time. A few exceptions allow human feedback to guide the selection of machine-trained models (Ross, Hughes, and Doshi-Velez 2017), including (Lage et al. 2018), which we discuss further in relation to human in the loop training. We are not aware of any work in this space which models humans in the machine training procedure.

**Humans in the loop.** Despite much recent interest in training with humans in the loop, experimentation in this setting remains an exceptionally challenging task. As mentioned above, Lage et al. (2018) is the only interpretability method we know of to directly incorporate human responses into training. There, the feedback mechanism is simple, and the authors explicitly abandon attempts to train with mTurkers, working instead with a group of machine learning graduate students and postdocs. Other work on human-machine cooperation proposes methods for training with humans, but either demonstrates results through fully synthetic experiments using simulated human responses (Madras, Pitassi, and Zemel 2018). Our framework directly optimizes for human performance by querying humans during training for their decisions on arbitrary points in representation space.

## 2 Method

In a typical setting, a decision-making user is given an *instance*  $x \in \mathcal{X}$ . For clarity, we will consider  $\mathcal{X} = \mathbb{R}^d$ . Given  $x$ , the user must decide on an *action*  $a \in \mathcal{A}$ . For example, if  $x$  are details of a loan application, then users can choose  $a \in \{\text{approve}, \text{deny}\}$ . Each instance is also associated with a ground-truth *outcome*  $y \in \mathcal{Y}$ , so that  $(x, y)$  is sampled from an unknown distribution  $D$ . We assume that users seek to choose actions that minimize an incurred *loss*  $\ell(y, a)$ , with  $\ell$  also known to the system designer; e.g., for loans,  $y$  denotes whether or not a person will repay the loan. We consider the general class of *prediction policy problems* (Kleinberg et al. 2015), where the loss function is known for a given action  $a$  and outcome  $y$ , and the difficulty in decision-making is governed by how well  $y$  can be predicted.

We denote by  $h$  the *human mapping* from inputs to decisions or actions. For example,  $a = h(x)$  denotes a decision based on raw instances  $x$ , but other sources of input such as *explanations*  $e$  or representations can be considered; e.g.,  $a = h(x, e)$  denotes a decision based on  $x$  and explanation  $e$ . The function  $h$  may output either a deterministic action or a probability distribution over actions. We conceptualize  $h$  as either representing a single human, or a stable distribution over a crowd of humans. We assume the mapping  $h$  is fixed (if there is adaptation to a representation,  $h$  can be thought of as the end-point of this adaptation).

Crucially, we allow machines to present users with machine-generated *advice*  $\gamma(x)$ , with human actions denoted as  $a = h(\gamma(x))$ . Users may additionally have access to *side information*  $s$  that is unavailable to the machine, in

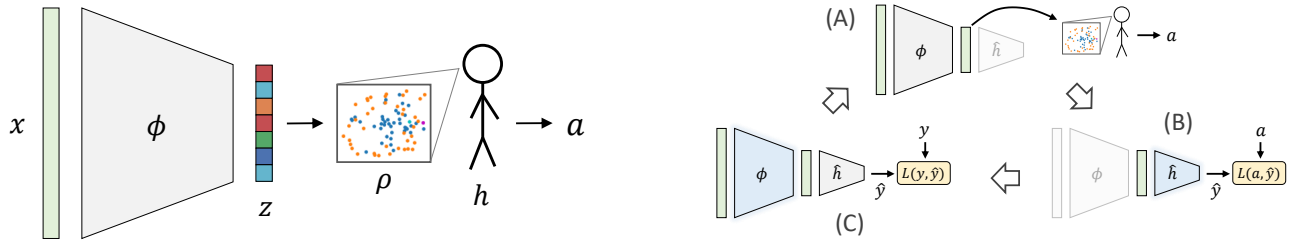


Figure 1: **Left:** The M◦M framework. The neural network learns a mapping  $\phi$  from inputs  $x$  to representations  $z$ , such that when  $z$  is visualized through  $\rho$ , representations elicit good human decisions. **Right:** Training alternates between (A) querying users for decisions on the current representations, (B) using these to train a proxy network  $\hat{h}$ , and (C) re-training representations.

which case user actions are  $a = h(\gamma(x), s)$ .<sup>1</sup> Advice  $\gamma(x)$  allows for a *human-centric representation* of the input, and we seek to *learn* a mapping  $\gamma$  from inputs to representations under which humans will make good decisions. The benchmark for evaluation will be the expected loss entailed by human actions given this advice:

$$\mathbb{E}_D[\ell(y, a)], \quad \text{for } a = h(\gamma(x)). \quad (1)$$

**Predictive advice.** A standard approach provides human users with machine-generated predictions,  $\hat{y} = f(x)$ , where  $f$  is optimized for predictive accuracy and the predictions themselves correspond to action recommendations (e.g., ‘will return loan’ corresponds to ‘approve loan’). This is a special case of our framework where advice  $\gamma = (x, \hat{y})$ , and the user is modeled as  $a = \hat{y} = h(x, \hat{y})$ . The predictive model is trained to minimize:

$$\min_f \mathbb{E}_D[\ell(y, \hat{y})], \quad \text{for } \hat{y} = f(x). \quad (2)$$

This makes plain that predictions  $f(x)$  are useful only to the extent that the human decision-maker follows them. Moreover, predictions provide only a scalar summary of the information in  $x$ , and limit the degree to which users can exercise their cognitive and decision-making capabilities; e.g., in the context of side information.

**Representational advice.** In M◦M, we allow advice  $\gamma$  to map inputs into representations that are designed to be suitably high-dimensional while also utilizing human strengths (e.g., a scatterplot, a compact linear model, or an avatar). Given a *representation class*,  $\Gamma$ , we seek a mapping  $\gamma \in \Gamma$  that minimizes expected loss  $\min_{\gamma \in \Gamma} \mathbb{E}_D[\ell(y, h(\gamma(x)))]$ . With a *training set*  $\mathcal{S} = \{(x_i, y_i)\}_{i=1}^m$  sampled from  $D$ , and with knowledge of the human mapping  $h$ , we would find a mapping  $\gamma$  minimizing the *empirical loss*:

$$\min_{\gamma \in \Gamma} \sum_{i=1}^m \ell(y_i, a_i), \quad \text{for } a_i = h(\gamma(x_i)), \quad (3)$$

possibly under some form of regularization. Here,  $\Gamma$  needs to be rich enough to contain flexible mappings from inputs

<sup>1</sup>This notion of machine-generated advice generalizes both explanations (as  $\gamma = (x, \hat{y}, e)$ , where  $e$  is the explanation) and deferrals (as  $\gamma = (x, \bar{y})$ , where  $\bar{y} \in \{0, 1, \text{defer}\}$ ), with a human model that always accepts  $\{0, 1\}$  (Madras, Pitassi, and Zemel 2018).

to representations, as well as to generate objects that are accessible to humans. To achieve this, we decompose this algorithmic advice  $\gamma(x) = \rho(\phi_\theta(x))$  into two components:

- $\phi_\theta : \mathbb{R}^d \rightarrow \mathbb{R}^k$  is a parametrized *embedding model* with learnable parameters  $\theta \in \Theta$ , that maps inputs into vector representations  $z = \phi_\theta(x) \in \mathbb{R}^k$  for some  $k > 1$
- $\rho : \mathbb{R}^k \rightarrow \mathcal{V}$  is a *visualization component* that maps each  $z$  into a visual object  $v = \rho(z) \in \mathcal{V}$  (e.g., a scatterplot, a facial avatar).

We consider different, fixed visualization components  $\rho$ , and focus on learning the embedding model  $\phi_\theta$ , and it is this question of embedding  $\phi_\theta$  that becomes the problem of learning representations in M◦M. Henceforth, it is convenient to fold the visualization component  $\rho$  into the human mapping  $h$ , and write  $h(z)$  to mean  $h(\rho(z))$ , for embedding  $z = \phi_\theta(x)$ . The training problem (3) becomes:

$$\min_{\theta \in \Theta} \sum_{i=1}^m \ell(y_i, a_i), \quad \text{for } a_i = h(\phi_\theta(x_i)), \quad (4)$$

again, perhaps with some regularization. By solving (4), we learn representations that promote good decisions by the human user. See Figure 1 (left).

**Training procedure, and human proxy.** We adopt a neural network to model the parametrized embedding  $\phi_\theta(x)$ , and thus advice  $\gamma$ . The main difficulty in optimizing (4) is that human actions  $\{a_i\}_{i=1}^m$  depend on  $\phi_\theta(x)$  via an unknown human mapping  $h$ . Hence, gradients of  $\theta$  must pass through  $h$ , but this function represents an actual human decision process. To handle this, we make use of a *differentiable proxy of the human mapping*,  $\hat{h}_\eta : \mathbb{R}^k \rightarrow \Gamma$ , parameterized by  $\eta \in H$ , which we learn. We refer to this as “h-hat.”

We learn using a *human-in-the-loop training procedure* that alternates between two steps:

1. Using the current  $\theta$  to gather samples of real human decisions  $a = h(z)$  on inputs  $z = \phi_\theta(x)$  and fitting  $\hat{h}_\eta$ .
2. Find  $\theta$  to optimize the performance of  $\hat{h}_\eta \circ \phi_\theta$  for the current  $\eta$ , as in (4).

Figure 1 (right) illustrates this process (for pseudocode see Appendix A). Since  $\hat{h}$  is trained to be locally rather than globally accurate,  $\hat{h}$  need not exactly match  $h$  for learning to improve. Rather, it suffices for  $\hat{h}$  to induce gradients of

the loss that improve performance (see Figure 7 in the Appendix).  $\hat{h}$  must be periodically retrained because as parameters  $\theta$  change, so does the induced distribution of representations  $z$ , and  $\hat{h}_\eta$  may become less accurate.

**Extensions.** One way in which humans can potentially surpass machines is when they have access to side information  $s$  that is informative of  $y$  yet unknown to the machine. The M◦M framework can be extended to learn a representation  $\gamma(x)$  that is optimal *conditional on the human using  $s$* , and despite lacking access to  $s$ . At test time, the human has access to  $s$ , and so action  $a = h(\phi(x), s)$ . At train time,  $y$  can be used as a proxy for  $s$ : if  $s$  is informative of  $y$ , then  $(x, y)$  are jointly informative of  $s$ . Although  $s$  cannot generally be reconstructed without supervision, in some cases  $(x, y)$  can be used to make inferences on  $s$ . As a simple example, consider the case where  $y = g(x, s)$  for some  $g$  and fix  $x$ . If  $g$  is invertible w.r.t.  $y$  for all  $x$ , then  $s$  can be fully reconstructed using  $g^{-1}(x, y)$ . In general,  $g$  may not be invertible, but a ‘lossy’ approximate inverse mapping  $\hat{g}^{-1}(x, y)$  can still be modeled into  $\hat{h}$ , now taking as input  $(z, x, y)$ .

### 3 Experimental Results

In this section, we report the results of three distinct experiments. Our intent is to demonstrate the breadth of the framework’s potential, and the experiments we present vary in the decision task, the form of representational advice, their complexity and scale, and the degree of human involvement (one experiment is entirely through simulations, another uses thousands of mTurk queries). We defer some of the experimental details to the Appendix.

#### 3.1 Decision-compatible scatterplots

In the first experiment, we focus on learning useful, low-dimensional representations of high-dimensional data, in the form of scatterplots. The choice of how to project high-dimensional data into a lower-dimensional space is consequential to decision-making (Kiselev, Andrews, and Hemberg 2019), and yet standard dimensionality-reduction methods optimize statistical criteria (e.g., maximizing directional variation in PCA) rather than optimizing for success in user interpretation. The M◦M framework learns projections that, once visualized, directly support good decisions.

We consider a setting where the goal is to correctly classify objects in  $p$ -dimensional space,  $p > 2$ . Each example  $x$  is a  $p$ -dimensional point cloud consisting of  $m = 40$  points in  $\mathbb{R}^p$  (so  $x \in \mathbb{R}^{40p}$ ). Point clouds are constructed such that, when orthogonally projected onto a particular linear 2D subspace of  $\mathbb{R}^p$ , denoted  $V$ , they form the shape of either an ‘X’ or an ‘O’, this determining their true label  $y$ . All directions orthogonal to  $V$  contain similarly scaled random noise.

Subjects are presented with a series of scatterplots, which visualize the point clouds for a given 2D projection, and are asked to determine for each point cloud its label (‘X’ or ‘O’). Whereas a projection onto  $V$  produces a useful representation, most others do not, including those learned coming from PCA. Our goal is to show that M◦M can use human feedback to learn a projection ( $\phi$ ) that produces visually meaningful scatterplots ( $\rho$ ), leading to good decisions.

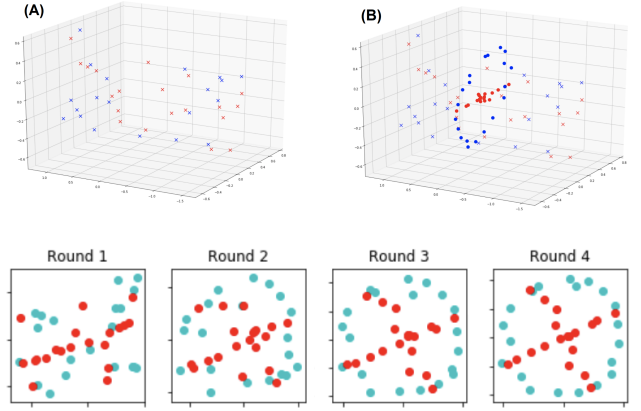


Figure 2: Low dimensional representations of point clouds. **(A)** Points in their original 3D representation give little visual indication of class (X or O). **(B)** Shapes become easily distinguishable when projected onto an appropriate subspace (shown in bold). **(Bottom)** Learned 2D representations after each training round. The initial 2D projection (round 1), on which a machine-classifier is fully accurate, is unintelligible to people. However, as training progresses, feedback improves the projection until the class becomes visually apparent (round 4), with very high human accuracy.

**Model.** Here, representation  $\phi$  plays the role of a dimensionality reduction mapping. We use  $d = 3$  and set  $\phi$  to be a  $3 \times 2$  linear mapping. The parameters  $\theta$  of mapping  $\phi$  are the entries of the  $3 \times 2$  matrix, and  $\phi$  is augmented with an orthogonality penalty  $\phi^T \phi - \mathbb{I}$  to encourage matrices which represent rotations. For the human proxy model, we want to be able to roughly model the visual perception of subjects. For this, we use for  $\hat{h}$  a small, single-layer  $3 \times 3$  convolutional network, that takes as inputs a soft (differentiable)  $6 \times 6$  histogram over the 2D projections.

**Results.** We recruited 12 computer science students to test the M◦M framework. Participants watched an instructional video and then completed a training and testing phase, each having five rounds (with intermittent model optimization) of 15 queries to label plots as either ‘X’ or ‘O’. The results we provide refer to the testing phase. Round 1 includes representations based on a random initialization of model parameters and therefore serves as a baseline condition. The results show that participants achieve an average accuracy of 68% in round 1, but improve to an average accuracy of 91% in round 5, a significant improvement of 23% ( $p < .01$ , paired  $t$ -test) with 75% of participants achieving 100% accuracy by round 5. Subjects are never given machine-generated predictions or feedback, and progress is driven solely by the performance of subjects on the reframed problem instances.

Figure 2 demonstrates a typical example of a five-round sequential training progression. Initially, representations produced by M◦M are difficult to classify when  $\theta$  is initialized arbitrarily. (This is also true when  $\theta$  is initialized with a fully accurate machine-only model.) As training progresses,

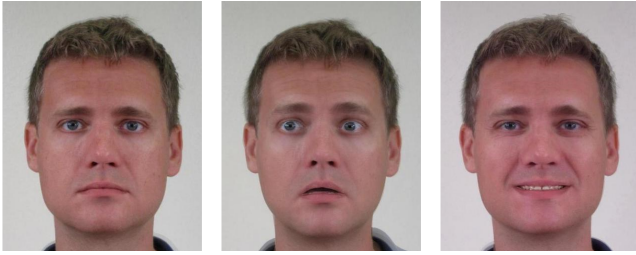


Figure 3: Different facial avatars, each avatar representing an algorithmic assistant and not a loan applicant, and trained to provide useful advice through facial expressions. The left-most avatar is set to a neutral expression ( $z = 0$ ).

feedback regarding subject perception gradually rotates the projection, revealing distinct class shapes. Training progress is made as long as subject responses carry some machine-discernible signal regarding the subject’s propensity to label a plot as ‘X’ or ‘O’. MoM utilizes these signals to update the representations and improve human performance.

### 3.2 Decision-compatible algorithmic avatars

For this experiment we consider a real decision task and use real data (approving loans), train with many humans participants (mTurkers), and explore a novel form of representational advice (facial avatars). Altogether we elicit around 6,000 human decisions for training and evaluation.<sup>2</sup> Specifically we use the *Lending Club* dataset, focusing on the resolved loans, i.e., loans that were paid in full ( $y = 1$ ) or defaulted ( $y = 0$ ), and only using features that would have been available to lenders at loan inception.<sup>3</sup> The decision task is to determine whether to approve a loan ( $a = 1$ ) or not ( $a = 0$ ), and the loss function we use is  $\ell(y, a) = \mathbb{1}_{\{y \neq a\}}$ .

**Goals, expectations, and limitations.** Whereas professional decision-makers are inclined to exercise their own judgment and deviate from machine advice (Stevenson and Doleac 2019; De-Arteaga, Fogliato, and Chouldechova 2020), mTurkers are non-experts and are likely to follow machine predictions (Lai and Tan 2018; Yin, Vaughan, and Wallach 2019).<sup>4</sup> For this reason, the goal of the experiment is *not to demonstrate performance superiority over purely predictive advice*, nor to show that mTurkers can become expert loan officers. Rather, the goal is to show that abstract representations can convey predictive advice in a way that requires users to deliberate to make a decision, and to explore whether humans use learned representations differently than they use machine predictions in making decisions. In Appendix B we further discuss the unique challenges encountered when training with mTurkers in the loop.

<sup>2</sup>All experiments are conducted subject to ethical review by the university’s IRB.

<sup>3</sup><https://www.kaggle.com/wendykan/lending-club-loan-data>

<sup>4</sup>We only know of Turk experiments in which good human performance from algorithmic advice can be attributed to humans accepting the advice of accurate machine predictions (Lai, Carton, and Tan 2020, e.g.).

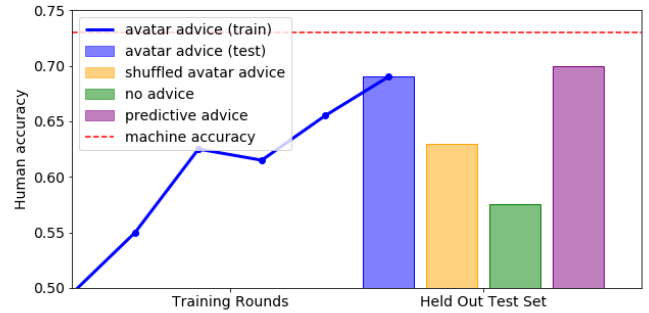


Figure 4: Human accuracy in the algorithmic advice condition (‘avatar advice’) consistently increases over rounds. Performance quickly surpasses the ‘no advice’ (data only) condition, and steadily approaches performance of users observing algorithmic predictions (‘predictive advice’), which in itself is lower than machine-only performance (‘machine accuracy’). Human accuracy falls when faces are shuffled within predicted labels of  $\hat{h}$ , confirming that faces convey useful, multi-variate information.

**Representations.** With the aim of exploring broader forms of representational advice, we make use of a *facial avatar*, framed to users as an *algorithmic assistant*—not the recipient of the loan—and communicating through its facial expressions information that is relevant to a loan decision. The avatar is based on a single, realistic-looking face capable of conveying versatile expressions (Figure 4 includes some examples). Expressions vary along ten dimensions including as *basic emotions* (Du, Tao, and Martinez 2014), *social dimensions* (e.g., dominance and trustworthiness (Du, Tao, and Martinez 2014; Todorov et al. 2008)), and subtle changes in *appearance* (e.g., eye gaze). Expressions are encoded by the representation vector  $z$ , with each entry corresponding to a different facial dimension. Thus, vectors  $z$  can be thought of as points in  $k$ -dimensional ‘face-space’ in which expressions vary smoothly with  $z$ .

We are interested in facial avatars because they are abstract (i.e., not in the domain of the input objects) and because they have previously been validated as useful representations of information (Chernoff 1973; Lott and Durbridge 1990). They are also high-dimensional representations, and non-linear in the input features; that is, faces are known to be processed holistically with dependencies beyond the sum of their parts (Richler et al. 2009). Faces also leverage innate human cognition—immediate, effortless, and fairly consistent processing of facial signals (Izard 1994; Todorov et al. 2008; Freeman and Johnson 2016).

Through MoM, we *learn* a mapping from inputs to avatars that is useful for decision-making. Training is driven completely by human responses, and learned expressions reflect usage patterns that users found to be useful, as opposed to the hand-coded mappings as used in *Chernoff faces* (Chernoff 1973). In a successful mapping, the avatars can summarize combinations of variables, but with the range and variation of expression calibrated such that *decision-relevant*



variation in the data is salient. In this way, learned avatars can relate data points to the full training set (e.g., encoding how extreme the values are).

**Model and training.** We set  $\phi$  to be a small, fully connected network with a single 25-hidden unit layer, mapping inputs to representation vectors  $z \in \mathbb{R}^9$ . The visualization component  $\rho(z)$  creates avatars by morphing a set of base images, each corresponding to a facial dimension, with  $z$  used to weight the importance of each base image.<sup>5,6</sup> We use a regularization term that, at the cost of some reduction in accuracy, encourages points in face-space to preserve distances in instance-space. As we will show, this promotes representations that carry more information about inputs than that implied by simple predictions. For  $\hat{h}$  we use a small, fully connected network with two layers of size 20 each, operating directly on representation vectors  $z$ .

In collecting human decisions for training  $\hat{h}$ , mTurkers were queried for their decisions regarding the approval or denial of loan applications.<sup>7</sup> New users were recruited at each round to obtain reports that are as independent as possible and to control for any human learning. Each user was queried for a random subset of 40 training examples, with the number of users chosen to ensure that each example would receive multiple responses (w.h.p.). For predictive purposes, binary outputs were set to be the majority human response. Each loan application was presented using the most informative features as well as the avatar. We did not relate to users any specific way in which they should incorporate avatar advice, and *care was taken to ensure users understood that the avatar represents an algorithmic assistant and not a loan applicant*.<sup>8</sup> Appendix C.2 provides further details regarding the experimental setup.

**Results.** Our results show that M◦M can learn representations that support good decisions through a complex, abstract representation, and that this representation carries multi-variate information, making it qualitatively different than prediction. As benchmarks, we consider the accuracy of a trained neural network model  $\mathcal{N}(x)$  having architecture equal to  $\hat{h} \circ \phi$  (but otherwise unrelated to our human-in-the-loop experiments), as well as human performance under predictive advice  $\gamma(x) = \tilde{y} \in [0, 1]$  where  $\tilde{y}$  is the predicted probability of  $\mathcal{N}(x)$ . We also consider a condition with ‘shuffled’ avatar advice, which we describe below.

Figure 4 shows the training process and resulting test accuracy (the data is balanced, with chance  $\approx 0.5$  accuracy).<sup>9</sup>

<sup>5</sup>Morphed images were created using the *Webmorph* software package (DeBruine and Tiddeman 2016).

<sup>6</sup>All base images correspond to the same human actor, whose corresponding avatar was used throughout the experiment.

<sup>7</sup>Recognizing that we use the same representation mapping for all users, we restrict to US-based participants to promote greater cross-user consistency with greater, common cultural understanding of face-space.

<sup>8</sup>Respondents who did not understand this point in a comprehension quiz were not permitted to complete the task.

<sup>9</sup>Results are statistically significant under a one-way ANOVA test,  $F(3, 196) = 2.98, p < 0.03$ .

At first, the (randomly-initialized) representation  $\phi$  produces arbitrary avatars, and performance in the avatar condition is lower than in the no-advice condition. This indicates that users take into account the (initially uninformative) algorithmic advice. As learning progresses, user feedback accumulates and the accuracy from using the M◦M framework steadily rises. After six rounds, avatar advice contributes to a boost of 11.5% in accuracy (0.69) over the no-advice condition (0.575), reaching 99% of the accuracy in the predictive advice condition (0.70). Performance in the predictive advice condition does not reach machine accuracy (0.73), showing that not all subjects follow predictive advice.

**Analysis.** We additionally explore what the representations learn, and how humans incorporate them into predictions. One possible concern is that despite regularization, learned avatars may simply convey binary predictions through fancy graphics (e.g., happy or sad faces). To explore this, we added a ‘shuffled’ condition in which faces are shuffled within predicted labels of  $\hat{h}$ . As shown in Figure 4, shuffling degrades performance and confirms that faces convey more complex information than the system’s binary prediction. Moreover, the avatars do not provide a simple encoding of a univariate (but not binary) prediction, and humans do not use the information in the same way that they use numeric predictions: (i) no single feature of  $z$  has a correlation with human responses  $\hat{h}(z)$  of more than  $R^2 = 0.7$ , (ii) correlations of average human response with the features of  $z$  are low (at most  $R^2 = 0.36$  across features) while responses in the predictive condition have  $R^2 = 0.73$  with the predictions, and (iii) users in the avatar condition self-report using the data as much or more than the advice 83% of the time, compared to 47% for the predictive advice condition.

At the same time,  $z$  preserves important information regarding  $x$ . To show this, we train linear models to predict from  $z$  each of the data features: interest rate (RATE), loan term (TERM), debt to income ratio (DTI), negative public records (REC), annual income (INC), employment length (EMP). Results show that  $z$  is highly informative of RATE ( $R^2 = 0.79$ ) and TERM (0.57), mildly informative of REC ( $-0.21$ ), INC (0.23), and EMP (0.13), and has virtually no predictive power of DTI ( $-0.03$ ). Further inspecting model coefficients reveals a complex pattern of how  $z$  carries information regarding  $x$  (see Appendix C.2 for all coefficients). For example: trustworthiness plays an important part in predicting all features, whereas anger is virtually unused; happiness and sadness do not play opposite roles—happiness is significant in TERM, while sadness is significant in RATE; and whereas EMP linked almost exclusively to age variation, INC is expressed by over half of the facial dimensions.

### 3.3 Incorporating side information

As an additional demonstration of the unique capabilities of M◦M we show that the framework can also learn representations that allow a decision maker to leverage side information that is unavailable to the machine. Referencing our earlier discussion of mTurk, we adopt simulation for this experiment because it is challenging for non-experts (like mTurkers) to outperform purely predictive advice and even

with access to additional side information. Simulation also allows us to systematically vary the synthetic human model, and we consider four distinct models of decision making.

The task we consider is a medical decision-making setting where doctors must evaluate the health risk of incoming ER patients, and have access to a predictive model.<sup>10</sup> Here, we focus on compact, linear models, and view the coefficients of the model along with the input features as the representation, affecting the decision process of doctors. Doctors also have access to additional, side information. Our goal is to learn a compact, linear model that can account for how doctors choose to use this side information.

**Setup.** There are four primary binary features  $x \in \{0, 1\}^4$ : diabetes ( $x_d$ ), cardiovascular disease ( $x_c$ ), race ( $x_r$ ), and income level ( $x_i$ ). An additional integer ‘side-information’ variable  $s \in \{0, 1, 2, 3\}$  encodes how long the patient’s condition was allowed to progress before coming to the ER and is available only to the doctor. We assume ground-truth risk  $y$  is determined only by diabetes, cardiovascular disease, and time to ER, through  $y = x_d + x_c + s$ , where  $x_d, x_c, s$  are sampled independently. We also assume that  $x_r$  and  $x_i$  jointly correlate with  $y$ , albeit not perfectly, so that they carry some but not all signal in  $s$  (whereas  $x_d, x_c$  do not, see Appendix C.3 for full details). In this way, race and income can be useful in prediction as they offer predictive power beyond that implied by their correlations with known health conditions (e.g., diabetes, cardiovascular disease), but interfere with how side information is used.

We model a decision maker who generally follows predictive advice  $\hat{y} = f_w(x) = \langle w, x \rangle$ , but with the capacity to adjust the machine-generated risk scores at her discretion and in a way that depends on the model through its coefficients  $w$ . We assume that doctors are broadly aware of the correlation structure of the problem, and are prone to incorporate the available side information  $s$  into  $\hat{y}$  if they believe this will give a better risk estimate. We model the decisions of a population of doctors as incorporating  $s$  additively and with probability that increases with the magnitude of either of the coefficients  $w_r$  and  $w_i$ . We refer to this as the *or* model and set  $h_{\text{or}}(x, s, w) = \hat{y} + I(w) \cdot s$  with  $I(w) \propto 1/(\max\{w_r, w_i\})$ , so that more weight on  $w_r$  and  $w_i$  reduces the probability of incorporating  $s$ . We also consider simpler decision models: *always* using side information ( $h_{\text{always}}$ ), *never* using side information ( $h_{\text{never}}$ ), and a *coarse* variant of  $h_{\text{or}}$  using binarized side information,  $h_{\text{coarse}} = \hat{y} + I(w) \cdot 2 \cdot \mathbb{1}\{s \geq 2\}$ .

**Model.** The representation  $\rho(z)$  consists of  $x$ , coefficients  $w$  (these are learned within  $\phi$ ), and  $\hat{y} = \langle w, x \rangle$ .<sup>11</sup> The difficulty in optimizing  $\phi$  is that  $s$  is never observed, and our proposed solution is to use  $y$  (which is known at train time) as a proxy for  $s$  when fitting  $\hat{h}$ , which is then used to train  $\phi$  (see Section 2). Since  $x$  and  $y$  jointly carry information regarding  $s$ , we define  $\hat{h}(x, y; w) = \langle w, x \rangle + \hat{s}(x, y)$ , where  $\hat{s}(x, y) = v_0 y + \sum_{j=1}^4 v_j x_j$ , and  $v$  are parameters. Note that

<sup>10</sup>MDCalc.com is one example of a risk assessment calculator for use by medical professionals.

<sup>11</sup>In an application, representations should also convey to users that the system is aware they may have additional side information.

Table 1: Performance of M◊M in the presence of side information and with four different synthetic human models. The machine-only performance is 0.890.

	M◊M	$h(\text{Machine})$
Or	1.0	.894
Coarse Or	.951	.891
Never	.891	.891
Always	1.0	.674

it is enough that  $\hat{s}$  models how the user *utilizes* side information, rather than the value of  $s$  directly;  $s$  is never observed, and there is no guarantee about the relation between  $\hat{s}$  and  $s$ .

**Results.** We compare M◊M to two other baselines: a machine-only linear regression, and the human model  $h$  applied to this machine-only model, and evaluate performance on the four synthetic human models ( $h_{\text{or}}$ ,  $h_{\text{coarse}}$ ,  $h_{\text{never}}$ , and  $h_{\text{always}}$ ). Both M◊M and the baselines use a linear model but the model in M◊M is trained to take into account how users incorporate side information. For evaluation, we consider binarized labels  $y_{\text{bin}} = \mathbb{1}\{y > 3\}$ .

We report results averaged over ten random data samples of size 1,000 with a 80-20 train-test split. As Table 1 shows, due to its flexibility in finding a representation that allows for incorporation of side information by the user, M◊M reaches 100% accuracy for the *or* and *always* decision models. M◊M maintains its advantage under the *coarse-or* decision model (i.e., when doctors use imperfect information), and remains effective in settings where side information is never used.

The problem with the baseline model is that it includes non-zero coefficients for all four features. This promotes accuracy in a machine-only setting, and in the absence of side information. Given this, the *or* and *coarse-or* decision models only very rarely introduce the side information—and this is indeed the best they can do given that the machine model uses all four variables. In contrast, for the *always* decision model the user always introduces side information, causing over-counting of the time to ER effect on patient outcomes (because of correlations between  $s$  and  $x_r$  and  $x_i$ ). In contrast, M◊M learns a linear model that is optimally responsive to the human decision maker. For example, including non-zero coefficients for only  $x_d$  and  $x_c$  in the case of the *or* decision model.

## 4 Discussion

We have introduced a novel learning framework for supporting human decision-making. Rather than viewing algorithms as experts, asked to explain their conclusions to people, we position algorithms as advisors whose goal is to help humans make better decisions while retaining human agency. The M◊M framework learns to provide representations of inputs that provide advice and promote good decisions. We demonstrate success in learning to support human decision models. We hope that by tapping into innate cognitive human strengths, learned representations can improve human-machine collaboration by prioritizing information, highlighting alternatives, and correcting biases.

## Ethics Statement

By incorporating the use of human judgment rather than encouraging human automation bias or simply automation, the kinds of methods suggested here have the potential to fail more gracefully than traditional decision support systems. Still, the idea of seeking to optimize for human decisions should not be considered lightly. It is our belief that a responsible and transparent deployment of models with “h-hat-like” components should encourage environments in which humans are aware of what information they provide about their thought processes. Unfortunately, this may not always be the case, and ethical, legal, and societal aspects of systems that are optimized to promote particular human decisions must be subject to scrutiny by both researchers and practitioners. If designed to correct for inadvertent user biases, for example, the system will first have to learn these biases, and this can be sensitive information and damaging to users if not properly managed. These kinds of issues are not specific to our framework and have been a concern of the HCI community as early as 1998 (Fogg 1998). The opportunities and dangers of our framework generally reflect those of the broader field of persuasive technology (Berdichevsky and Neuenschwander 1999), where system goals may be poor proxies for user goals (Ribeiro et al. 2020), or even at odds with user goals. Moreover, the method does not in itself prevent biases from being passed through the data without appropriate care in the design of loss functions.

## References

- Angelino, E.; Larus-Stone, N.; Alabi, D.; Seltzer, M.; and Rudin, C. 2017. Learning certifiably optimal rule lists. In *Proc. 23rd ACM SIGKDD Int. Conference on Knowledge Discovery and Data Mining*, 35–44. ACM.
- Bandura, A. 1989. Human agency in social cognitive theory. *American psychologist* 44(9): 1175.
- Bandura, A. 2010. Self-efficacy. *The Corsini encyclopedia of psychology* 1–3.
- Bansal, G.; Nushi, B.; Kamar, E.; Lasecki, W. S.; Weld, D. S.; and Horvitz, E. 2019. Beyond Accuracy: The Role of Mental Models in Human-AI Team Performance. In *Proc. AAAI Conf. on Human Comput. and Crowdsourcing*.
- Barabas, C.; Dinakar, K.; Ito, J.; Virza, M.; and Zittrain, J. 2017. Interventions over predictions: Reframing the ethical debate for actuarial risk assessment. *arXiv preprint arXiv:1712.08238*.
- Berdichevsky, D.; and Neuenschwander, E. 1999. Toward an ethics of persuasive technology. *Comm. ACM* 42(5): 51–58.
- Bourgin, D. D.; Peterson, J. C.; Reichman, D.; Griffiths, T.; and Russell, S. J. 2019. Cognitive model priors for predicting human decisions. *arXiv preprint arXiv:1905.09397*.
- Brown, J. R.; Kling, J. R.; Mullainathan, S.; and Wrobel, M. V. 2013. Framing lifetime income. Technical report, National Bureau of Economic Research.
- Chernoff, H. 1973. The use of faces to represent points in k-dimensional space graphically. *JASA* 68(342): 361–368.
- Cosmides, L.; and Tooby, J. 1992. Cognitive adaptations for social exchange. *The adapted mind: Evolutionary psychology and the generation of culture* 163: 163–228.
- De-Arteaga, M.; Fogliato, R.; and Chouldechova, A. 2020. A Case for Humans-in-the-Loop: Decisions in the Presence of Erroneous Algorithmic Scores. In *Proc. 2020 CHI Conf. on Human Factors in Computing Systems*, 1–12.
- DeBruine, L.; and Tiddeman, B. 2016. Webmorph.
- Dietvorst, B. J.; Simmons, J. P.; and Massey, C. 2015. Algorithm aversion: People erroneously avoid algorithms after seeing them err. *Journal of Experimental Psychology: General* 144(1): 114.
- Dietvorst, B. J.; Simmons, J. P.; and Massey, C. 2016. Overcoming algorithm aversion: People will use imperfect algorithms if they can (even slightly) modify them. *Management Science* 64(3): 1155–1170.
- Doshi-Velez, F.; and Kim, B. 2017. Towards a rigorous science of interpretable machine learning. *arXiv preprint arXiv:1702.08608*.
- Du, S.; Tao, Y.; and Martinez, A. M. 2014. Compound facial expressions of emotion. *Proceedings of the National Academy of Sciences* 111(15): E1454–E1462.
- Elmalech, A.; Sarne, D.; Rosenfeld, A.; and Erez, E. S. 2015. When suboptimal rules. In *Twenty-Ninth AAAI Conference on Artificial Intelligence*.
- Engelbart, D. C. 1962. Augmenting human intellect: A conceptual framework. *Menlo Park, CA*.
- Esteva, A.; Kuprel, B.; Novoa, R. A.; Ko, J.; Swetter, S. M.; Blau, H. M.; and Thrun, S. 2017. Dermatologist-level classification of skin cancer with deep neural networks. *Nature* 542(7639): 115.
- Fogg, B. J. 1998. Persuasive computers: perspectives and research directions. In *Proceedings of the SIGCHI conference on Human factors in computing systems*, 225–232.
- Freeman, J. B.; and Johnson, K. L. 2016. More than meets the eye: Split-second social perception. *Trends in cognitive sciences* 20(5): 362–374.
- Gigerenzer, G.; and Hoffrage, U. 1995. How to improve Bayesian reasoning without instruction: frequency formats. *Psychological review* 102(4): 684.
- Green, B.; and Chen, Y. 2019a. Disparate interactions: An algorithm-in-the-loop analysis of fairness in risk assessments. In *Proc. ACM FAT Conf. ACM*.
- Green, B.; and Chen, Y. 2019b. The principles and limits of algorithm-in-the-loop decision making. *Proceedings of the ACM on Human-Computer Interaction* 3(CSCW): 1–24.
- Izard, C. E. 1994. Innate and universal facial expressions: Evidence from developmental and cross-cultural research. *Psychological Bulletin* 115(2): 288–299.
- Kahneman, D. 2011. *Thinking, fast and slow*. Macmillan.
- Kahneman, D.; and Tversky, A. 2013. Prospect theory: An analysis of decision under risk. In *Handbook of the fundamentals of financial decision making: Part I*, 99–127. World Scientific.



- Kiselev, V. Y.; Andrews, T. S.; and Hemberg, M. 2019. Challenges in unsupervised clustering of single-cell RNA-seq data. *Nature Reviews Genetics* 20(5): 273–282.
- Kleinberg, J.; Ludwig, J.; Mullainathan, S.; and Obermeyer, Z. 2015. Prediction policy problems. *American Economic Review* 105(5): 491–95.
- Lage, I.; Chen, E.; He, J.; Narayanan, M.; Kim, B.; Gershman, S.; and Doshi-Velez, F. 2019. An evaluation of the human-interpretability of explanation. *arXiv preprint arXiv:1902.00006*.
- Lage, I.; Ross, A.; Gershman, S. J.; Kim, B.; and Doshi-Velez, F. 2018. Human-in-the-loop interpretability prior. In *Adv. in Neural Info. Proc. Sys.*, 10159–10168.
- Lai, V.; Carton, S.; and Tan, C. 2020. Harnessing Explanations to Bridge AI and Humans. *arXiv preprint arXiv:2003.07370*.
- Lai, V.; and Tan, C. 2018. On Human Predictions with Explanations and Predictions of Machine Learning Models: A Case Study on Deception Detection. *arXiv preprint arXiv:1811.07901*.
- Lakkaraju, H.; Bach, S. H.; and Leskovec, J. 2016. Interpretable decision sets: A joint framework for description and prediction. In *Proc. 22nd ACM SIGKDD Int. Conf. on Know. Disc. and Data Mining*, 1675–1684. ACM.
- Lakkaraju, H.; Kamar, E.; Caruana, R.; and Leskovec, J. 2019. Faithful and customizable explanations of black box models. In *Proceedings of the 2019 AAAI/ACM Conference on AI, Ethics, and Society*, 131–138. ACM.
- Lei, T.; Barzilay, R.; and Jaakkola, T. S. 2016. Rationalizing Neural Predictions. In *Proc. Conf. on Empirical Methods in Natural Language Processing*, 107–117.
- Licklider, J. C. R. 1960. Man-computer symbiosis. *IRE transactions on human factors in electronics* 4–11.
- Liu, X.; Faes, L.; Kale, A. U.; Wagner, S. K.; Fu, D. J.; Bruynseels, A.; Mahendiran, T.; Moraes, G.; Shamdass, M.; Kern, C.; et al. 2019. A comparison of deep learning performance against health-care professionals in detecting diseases from medical imaging: a systematic review and meta-analysis. *The Lancet Digital Health* 1(6): e271–e297.
- Logg, J. M. 2017. Theory of Machine: When do people rely on algorithms?
- Lott, J. A.; and Durbridge, T. C. 1990. Use of Chernoff faces to follow trends in laboratory data. *Journal of clinical laboratory analysis* 4(1): 59–63.
- Lundberg, S. M.; and Lee, S.-I. 2017. A unified approach to interpreting model predictions. In *Advances in Neural Information Processing Systems*.
- Madras, D.; Pitassi, T.; and Zemel, R. 2018. Predict Responsibly: Improving Fairness and Accuracy by Learning to Defer. In *Adv. in Neural Info. Proc. Sys.* 31, 6147–6157.
- Miller, G. A. 1956. The magical number seven, plus or minus two: Some limits on our capacity for processing information. *Psychological review* 63(2): 81.
- Nickerson, D. W.; and Rogers, T. 2014. Political campaigns and big data. *J. Econ. Persp.* 28(2): 51–74.
- Parikh, R. B.; Obermeyer, Z.; and Navathe, A. S. 2019. Regulation of predictive analytics in medicine. *Science* 363(6429): 810–812.
- Poursabzi-Sangdeh, F.; Goldstein, D. G.; Hofman, J. M.; Vaughan, J. W.; and Wallach, H. 2018. Manipulating and measuring model interpretability. *arXiv preprint arXiv:1802.07810*.
- Ribeiro, M. H.; Ottoni, R.; West, R.; Almeida, V. A.; and Meira Jr, W. 2020. Auditing radicalization pathways on youtube. In *Proc. ACM Conf. FAT*, 131–141.
- Ribeiro, M. T.; Singh, S.; and Guestrin, C. 2016. Why should i trust you?: Explaining the predictions of any classifier. In *Proc. 22nd ACM SIGKDD Int. Conf. on Know. Disc. and Data Mining*, 1135–1144. ACM.
- Richler, J. J.; Mack, M. L.; Gauthier, I.; and Palmeri, T. J. 2009. Holistic processing of faces happens at a glance. *Vision research* 49(23): 2856–2861.
- Ross, A. S.; Hughes, M. C.; and Doshi-Velez, F. 2017. Right for the right reasons: Training differentiable models by constraining their explanations. *arXiv preprint arXiv:1703.03717*.
- Smilkov, D.; Thorat, N.; Kim, B.; Viégas, F.; and Wattenberg, M. 2017. Smoothgrad: removing noise by adding noise. *arXiv preprint arXiv:1706.03825*.
- Stevenson, M.; and Doleac, J. 2018. Algorithmic Risk Assessment Tools in the Hands of Humans.
- Stevenson, M. T.; and Doleac, J. L. 2019. Algorithmic Risk Assessment in the Hands of Humans. *SSRN*.
- Sutton, R. T.; Pincock, D.; Baumgart, D. C.; Sadowski, D. C.; Fedorak, R. N.; and Kroeker, K. I. 2020. An overview of clinical decision support systems: benefits, risks, and strategies for success. *NPJ Digital Medicine* 3(1): 1–10.
- Thompson, P. 1980. Margaret Thatcher: A new illusion. *Perception*.
- Todorov, A.; Said, C. P.; Engell, A. D.; and Oosterhof, N. N. 2008. Understanding evaluation of faces on social dimensions. *Trends in cognitive sciences* 12(12): 455–460.
- Venkatesh, V.; Morris, M. G.; Davis, G. B.; and Davis, F. D. 2003. User acceptance of information technology: Toward a unified view. *MIS quarterly* 425–478.
- West, S.M. Whittaker, M.; and Crawford, K. 2019. Discriminating Systems: Gender, Race and Power in AI. URL <https://ainowinstitute.org/discriminatingystems.html>.
- Yeomans, M.; Shah, A.; Mullainathan, S.; and Kleinberg, J. 2017. Making sense of recommendations. *Journal of Behavioral Decision Making*.
- Yin, M.; Vaughan, J. W.; and Wallach, H. M. 2019. Understanding the Effect of Accuracy on Trust in Machine Learning Models. In *Proceedings of the 2019 Conference on Human Factors in Computing Systems*.

## Appendix A Optimization Algorithm

---

### Algorithm 1 Alternating optimization algorithm

---

```

1: Initialize  $\theta = \theta_0$ 
2: repeat
3:    $x_1, \dots, x_n \sim \mathcal{S}$   $\triangleright$  Sample  $n$  train examples
4:    $z_i \leftarrow \phi_\theta(x_i) \ \forall i \in [n]$   $\triangleright$  Generate representations
5:    $a_i \leftarrow h(\rho(z_i)) \ \forall i \in [n]$   $\triangleright$  Query human decisions
6:    $\mathcal{T} = \{(z_i, a_i)\}_{i=1}^n$ 
7:    $\eta \leftarrow \operatorname{argmin}_{\eta'} \mathbb{E}_{\mathcal{T}}[\ell(a, \hat{h}_{\eta'}(z))] \quad \triangleright$  Train  $\hat{h}$ 
8:    $\theta \leftarrow \operatorname{argmin}_{\theta'} \mathbb{E}_{\mathcal{S}}[\ell(y, \hat{h}_\eta(\phi_{\theta'}(x)))] \quad \triangleright$  Train  $\phi$ 
9: until convergence

```

---

## Appendix B General Optimization Issues

### B.1 Initialization

Because acquiring human labels is expensive, it is important to initialize  $\phi$  to map to a region of the representation space in which there is variation and consistency in human reports, such that gradients lead to progress in subsequent rounds.

In some representation spaces, such as our 2D projections of noisy 3D rotated images, this is likely to be the case (almost any 3D slice will retain some signal from the original 2D image). However, in 4+ dimensions, as well as with the subset selection and avatar tasks, there are no such guarantees.

To minimize non-informative queries, we adopt two initialization strategies:

1. **Initialization with a computer-only model:** In scenarios in which the representation space is a (possibly discrete) subset of input space, such as in subset selection, the initialization problem is to isolate the region of the input space that is important for decision-making. In this situation, it can be useful to initialize with a computer-only classifier. This classifier should share a representation-learning architecture with  $\phi$  but can have any other classifying architecture appended (although simpler is likely better for this purpose). This should result in some  $\phi$  which at least focuses on the features relevant for classification, if not necessarily in a human-interpretable format.

### B.2 Convergence

As is true in general of gradient descent algorithms, the M◦M framework is not guaranteed to find a global optimum but rather is likely to end up at a local optimum dependent on both the initialization of  $\phi$  and  $\hat{h}$ . In our case, however, the path of gradient descent is also dependent on the inherently stochastic selection and behavior of human users. If users are inconsistent or user groups at different iterations are not drawn from the same behavior distribution, it is possible that learning at one step of the algorithm could result in convergence to a suboptimal distribution for future users. It remains for future work to test how robust machine learning methods might be adapted to this situation to mitigate this issue.

### B.3 Regularization/Early Stopping

As mentioned in Section 2, training  $\phi$  will in general shift the distribution of the representation space away from the region on which we have collected labels for  $\hat{h}$  in the previous iterations, resulting in increasing uncertainty in the predicted outcomes. We test a variety of methods to account for this, but developing a consistent scheme for choosing how best to maximize the information in human labels remains future work.

- **Regularization of  $\hat{h}$ :** We test regularization of  $\hat{h}$  both with Dropout and L2 regularization, both of which help in preventing overfitting, especially in early stages of training, when the representation distribution is not yet refined. As training progresses and the distribution  $\phi_\theta(x)$  becomes more tightly defined, decreasing these regularization parameters increases performance.
- **Training  $\hat{h}$  with samples from previous iterations:** We also found it helpful in early training iterations to reuse samples from the previous human labeling round in training  $\hat{h}$ , as inspired by [Bobu et al. 2018].<sup>12</sup> We weight these samples equally and use only the previous round, but it may be reasonable in other applications to alter the weighting scheme and number of rounds used.
- **Early stopping based on Bayesian Linear Regression:** In an attempt to quantify how the prediction uncertainty changes as  $\theta$  changes, we also implement Bayesian Linear Regression, found in [Riquelme et al., 2018]<sup>13</sup> to be a simple but effective measure of uncertainty, over the last layer of  $\hat{h}(\phi_\theta)$  as we vary  $\theta$  through training. We find that in early iterations of training, this can be an effective stopping criterion for training of  $\phi$ . Again, as training progresses, we find that this mostly indicates only small changes in model uncertainty.

### B.4 Human Input

Testing on mTurk presents various challenges for testing the M◦M framework:

- In some applications, such as loan approval, mTurk users are not experts. This makes it difficult to convince them that anything is at stake (we found that bonuses did not meaningfully affect performance). It is also difficult to directly measure effort, agency, trust, or autonomy, all of which result in higher variance in responses.
- In many other applications, the ground truth is generated by humans to begin with (for example, sentiment analysis). Since we require ground truth for training, in these task it cannot be expected of humans to outperform machines.
- As the researchers found in (Lage et al. 2018), there can be a large variance in the time users take to complete a given task. Researchers have found that around 25% of

<sup>12</sup>Bobu, Andreea, et al. "Adapting to continuously shifting domains." (2018).

<sup>13</sup>Riquelme, Carlos, George Tucker, and Jasper Snoek. "Deep bayesian bandits showdown." *International Conference on Learning Representations*. 2018.

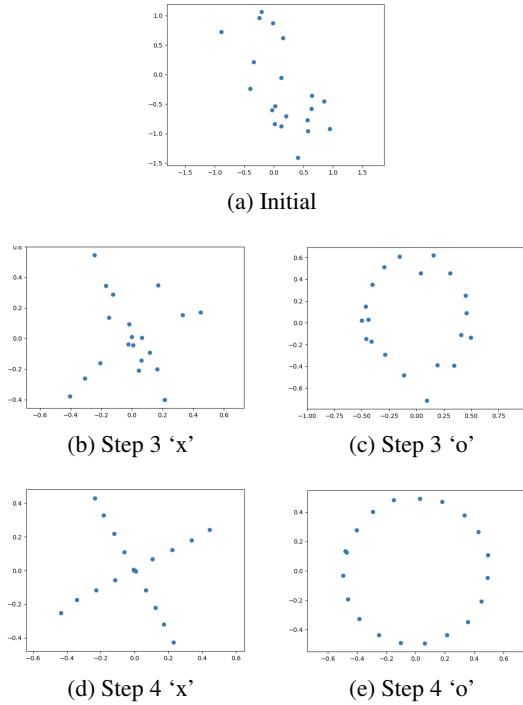


Figure 5: Images of x-o interface

mTurk users complete several tasks at once or take breaks during HITs [Moss and Litman, 2019].<sup>14</sup> making it difficult to determine how closely Turkers are paying attention to a given task. We use requirements of HIT approval rate greater than 98%, US only, and at least 5,000 HITs approved, as well as a simple comprehension check.

- Turker populations can vary over time and within time periods, again leading to highly variable responses, which can considerably effect the performance of learning.
- Recently, there have been concerns regarding the usage of automated bots within the mTurk community. Towards this end, we incorporated in the experimental survey a required reading comprehension task and as well as a CAPTCHA task, and filtered users that did not succeed in these.

## Appendix C Experimental Details

### C.1 Decision-compatible 2D projections

In the experiment, we generate 1,000 examples of these point clouds in 3D. The class of  $\phi$  is a  $3 \times 3$  linear layer with no bias, where we add a penalization term on  $\phi^T \phi - \mathbb{I}$  during training to constrain the matrix to be orthogonal. Humans are shown the result of passing the points through this layer and projecting onto the first two dimensions. The class of  $\hat{h}$  is a small network with 1  $3 \times 3$  convolutional layer creating 3 channels,  $2 \times 2$  max pooling, and a sigmoid over a final linear

<sup>14</sup>A. J. Moss and L. Litman. How do most mturk workers work?, Mar 2019.

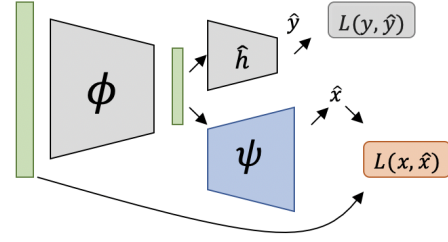


Figure 6: Visualization of reconstruction component

layer. The input to this network is a soft (differentiable)  $6 \times 6$  histogram over the 2D projection shown to the human user.

We tested an interactive command line query and response game on 12 computer science students recruited on Slack and email. Users filled out a consent form online, watched an instructional video, and then completed a training and testing round, each with up to 5 rounds of 15 responses. Due to the nature of the training process, achieving 100% accuracy results in  $\phi$  not updating in the following round. With this in mind, if a user reached 100% accuracy in training, they immediately progressed to testing. If a user reached 100% accuracy in testing, the program exited.  $\phi$  was able to find a representation that allowed for 100% accuracy 75% of the time, with an average 5 round improvement of 23% across all participants. Many times the resulting projection appeared to be an ‘x’ and ‘o’, as in Figure 5, but occasionally it was user-specific. For example, a user who associates straight lines with the ‘x’ may train the network to learn any projection for ‘x’ that includes many points along a straight line.

The architecture of  $\phi$  and  $\hat{h}$  are described in Section 3. For training, we use a fixed number of epochs (500 for  $\hat{h}$  and 300 for  $\phi$ ) with base learning rates of .07 and .03, respectively, that increase with lower accuracy scores and decrease with each iteration. We have found these parameters to work well in practice, but observed that results were not sensitive to their selection. The interface allows the number of rounds and examples to be determined by the user, but often 100% accuracy can be achieved after about 5 rounds of 15 examples each.

### C.2 Decision-compatible algorithmic avatars

**Data Preprocessing.** We use the *Lending Club* dataset, which we filter to include only loans for which we know the resolution (either default or paid in full, not loans currently in progress) and to remove all features that would not have been available at funding time. We additionally drop loans that were paid off in a single lump sum payment of at least 5 times the normal installment. This results in a dataset that is 49% defaulted and 51% repaid loans. Categorical features are transformed to one-hot variables. There are roughly 95,000 examples remaining in this dataset, of which we split 20% into the test set.

**Learning architecture and pipeline.** The network  $\phi$  takes as input the standardized loan data. Although the number of output dimension are  $\mathbb{R}^9$ ,  $\phi$  outputs vectors in  $\mathbb{R}^{11}$ . This is because the some facial expressions do not naturally coexist as compound emotions, i.e., happiness and sadness [Du et al., 2014].<sup>15</sup> Hence, we must add some additional constraints to the output space, encoded in the extra dimensions. For example, happiness and sadness are split into two separate parameters (rather than using one dimension with positive for happiness and negative for sadness). The same is true of “happy surprise”, which is only allowed to coincide with happiness, as opposed to “sad surprise.” For parameters which have positive and negative versions, we use a tanh function as the final nonlinearity, and for parameters which are positive only, we use a sigmoid function as the final nonlinearity.

These parameters are programmatically mapped to a series of Webmorph (DeBruine and Tiddeman 2016) transformation text files, which are manually loaded into the batch transform/batch edit functions of Webmorph. We use base emotion images from the CFEE database [Du et al., 2014] and trait identities from [Oosterhof and Todorov, 2008].<sup>16</sup> This forms  $\rho$  for this experiment.

The network  $\phi$  is initialized with a WGAN to match a distribution of parameters chosen to output a fairly uniform distribution of feasible faces. To achieve this, each parameter was chosen to be distributed according to one of the following: a clipped  $\mathcal{N}(0, 4)$ ,  $\mathcal{U}[0, 1]$ , or  $\text{Beta}(1, 2)$ . The choice of distribution was based on inspection as to what would give reasonable coverage over the set of emotional representations we were interested in testing. In this initial version of  $\phi$ ,  $x$  values end up mapped randomly to representations, as the WGAN has no objective other than distribution matching.

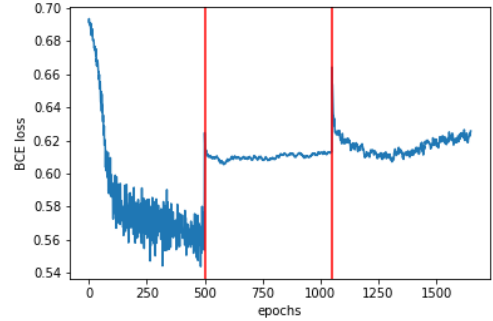
The hidden layer sizes of  $\phi$  and  $\hat{h}$  were chosen via cross validation. For  $\phi$ , we use the smallest architecture out of those tested capable of recreating a wide distribution of representations  $z$  as the generator of the WGAN. For  $\hat{h}$ , we use the smallest architecture out of those tested that achieves low error both in the computer-only simulation and with the first round of human responses.

In the first experiment, we collect approximately 5 labels each (with minor variation due to a few mTurk users dropping out mid-experiment) for the LASSO feature subset of 400 training set  $x$  points and their  $\phi_0$  mappings (see Figure 9).  $a$  is taken to be the percentage of users responding “approve” for each point.

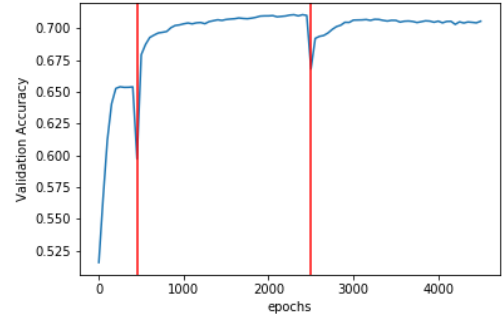
To train  $\hat{h}$ , we generate 15 different training-test splits of the collected  $\{z, a\}$  pairs and compare the performance of variations of  $\hat{h}$  in which it is either initialized randomly or with the  $\hat{h}$  from the previous iteration, trained with or without adding the samples from the previous iteration, and rang-

<sup>15</sup>Shichuan Du, Yong Tao, and Aleix M Martinez. Compound facial expressions of emotion. *Proceedings of the National Academy of Sciences*, 111(15):E1454–E1462, 2014.

<sup>16</sup>Nikolaas N Oosterhof and Alexander Todorov. The functional basis of face evaluation. *Proceedings of the National Academy of Sciences*, 105(32):11087–11092, 2008.



(a) Loss in training  $\hat{h}$  over 3 rounds



(b) Validation Accuracy in training  $\phi$  over 3 rounds

Figure 7:  $\hat{h}$  does not necessarily have to match  $h$  well to lead to an increase in accuracy

ing over different regularization parameters. We choose the training parameters and number of training epochs which result in the lowest average error across the 15 random splits. In the case of random initialization, we choose the best out of 30 random seeds over the 15 splits.

To train  $\phi$ , we fix  $\hat{h}$  and use batches of 30,000 samples per epoch from the training set, which has 75,933 examples in total. To prevent mode collapse, wherein faces “binarize” to two prototypical exemplars, we add a reconstruction regularization term  $R(x) = \|x - \psi(\phi(x))\|_2^2$  to the binary cross entropy accuracy loss, where  $\psi$  is a decoder implemented by an additional neural network (see Figure 6).  $\phi$  here also features a constraint penalty that prevents co-occurrence of incompatible emotions.

We train  $\phi$  for 2,000 epochs with the Adam optimizer for a variety of values of  $\alpha$ , where we use  $\alpha$  to balance reconstruction and accuracy loss in the form  $\mathcal{L}_{total} = \alpha\mathcal{L}_{acc} + (1 - \alpha)\mathcal{L}_{rec}$ . We choose the value of  $\alpha$  per round that optimally retains  $x$  information while promoting accuracy by inspecting the accuracy vs. reconstruction MSE curve. We then perform Bayesian Linear Regression over the final layer of the current  $\hat{h}$  for every 50th epoch of  $\phi$  training and select the number of epochs to use by the minimum of either 2,000 epochs or the epoch at which accuracy uncertainty has doubled. In all but the first step, this resulted in using 2,000

epochs.

At each of the 2-5th epochs, we choose only 200 training points to query. In the 6th epoch we use 200 points from the test set.

**Self-reported user type.** In the end of the survey, we ask users to report their decision method from among the following choices:

- I primarily relied on the data available
- I used the available data unless I had a strong feeling about the advice of the computer system
- I used both the available data and the advice of the computer system equally
- I used the advice of the computer system unless I had a strong feeling about the available data
- I primarily relied on the advice of the computer system
- Other

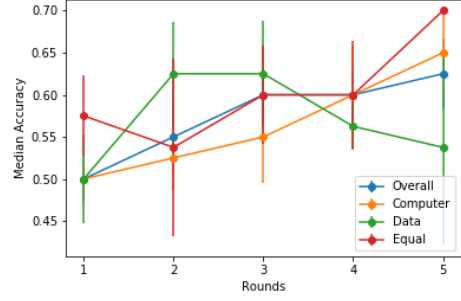
The percentage of users in each of these groups varied widely from round to round.

We consider the first two conditions to be the ‘Data’ group, the third to be the ‘Equal’ group, and the next two to be the ‘Computer Advice’ group. Although the trend is not statistically significant (at  $p = 0.05$ ), likely due to the small number of subjects per type per round, we find it interesting that the performance improved on average over training rounds for all three types, of which the equal-consideration type performed best. For the data-inclined users, whose performance improved to surpass that of the no-advice condition in as early as round two, this implies at least one of the following: users misreport their decision method; users believe they are not influenced by the advice but are in fact influenced; or, as the algorithmic evidence becomes apparently better, only the population of users who are comparatively skilled at using the data continue to do so.

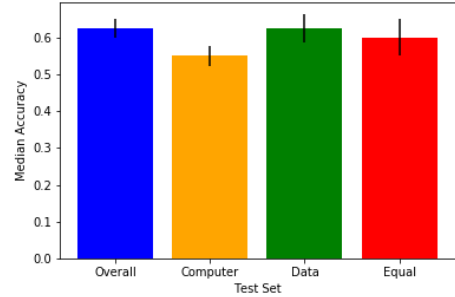
**Diversity in avatar representation.** We believe the additional dimensionality of the avatar representation relative to a numerical or binary prediction of default is useful for two reasons. Most importantly, high dimensionality allows users to retain an ability to reason about their decisions. In particular, avatars are useful because people likely have shared, mental reference points for faces. Moreover, users with a more sophisticated mental reference space may be able to teach the advising system over time to match specific reasoning patterns to specific characteristics. Additionally, when the advising system does not have a strong conviction about a prediction, presenting neutral advice should encourage the user to revisit the data, whereas percentages above or below the base rate of default (or 50%) may suffer from the anchoring effect.

**Further Details on Information Learned by  $z$ .** Using cross-validated ridge regression to predict individual  $x$  variables from individual  $z$  variables results in the coefficients of determination  $R^2$  (to 2 significant figures) shown in Table 2.

Using cross-validated ridge regression to predict individual  $x$  variables from all  $z$  variables (both standardized to mean 0, std 1) results in the *variable coefficients* (to 2 significant figures) shown in Table 3.



(a) Training Rounds (‘Overall’ here is average *per user* score, rather than the score of the average response per question)



(b) Test Round

Figure 8: Results by Reported User Type

### C.3 Incorporating Side Information

**Data Generation.** A directed graph showing the variable correlations is shown in Figure 10. The data in the side-information experiment is generated as follows: A latent variable  $l_0 \sim \mathcal{N}(.3, .1)$  introduces a low correlation between  $x_i$  and  $x_r$  by setting a common mean for their Bernoulli probabilities  $l_1, l_2$ :

- $l_1, l_2 \sim \text{Unif}(\max(l_0 - .3, 0), \min(l_0 + .3, 1))$
- $x_i \sim \text{Bernoulli}(1 - l_1)$
- $x_r \sim \text{Bernoulli}(1 - l_2)$

An additional latent variable  $l_3$  provides a similar correlation between  $x_c$  and  $x_d$ , which also correlate, respectively, with  $x_i$  and  $x_r$ :

- $l_3 \sim \text{Unif}(.5, .7)$
- $x_c \sim \text{Bernoulli}(l_3 + x_i)$
- $x_d \sim \text{Bernoulli}(l_3 + x_r)$

Side information  $s$  is highly correlated with  $x_r$  and  $x_i$  but noisy:  $s$  is drawn from a normal distribution centered at  $x_r + x_i$  before rounding to an integer value between 0 and 3.

- $s_{cont} \sim \mathcal{N}(x_r + x_i, .5)$
- $s = \max(0, \min(3, \text{round}(s_{cont})))$

The integer outcome variable  $y$  is the sum of  $x_c$ ,  $x_d$ , and  $s$ . The binary outcome variable  $y_{bin}$  is thresholded at  $y > 3$ .  
 $y = x_c + x_d + s$ ;  $y_{bin} = \mathbb{1}\{y > 3\}$

Table 2: Coefficients of Determination  $R^2$ , predicting each  $x$  variable from each final  $z$  variable.

	RATE	TERM	DT	REC	INC	EMP
happiness	0.00	-0.15	-0.14	0.00	-0.01	0.00
sadness	-0.01	-0.06	-0.10	0.00	-0.04	-0.07
trustworthiness	0.57	0.17	0.01	0.00	-0.01	-0.01
dominance	0.00	-0.01	0.03	-0.01	0.01	-0.01
hue	0.48	0.29	-0.02	0.00	-0.04	-0.02
eye gaze	0.42	0.46	-0.04	-0.40	-0.04	-0.17
age	0.23	0.22	-0.12	-0.21	0.17	0.04
anger	-0.01	-0.02	-0.05	-0.02	-0.01	0.00
fear	0.04	0.00	-0.03	0.00	-0.01	-0.01
surprise	-0.18	0.04	-0.01	-0.02	0.00	-0.04

Table 3: Coefficients of Ridge Regression, predicting each  $x$  variable from all final  $z$  variables.

	RATE	TERM	DT	REC	INC	EMP
happiness	-0.07	-0.29	-0.10	-0.06	0.21	-0.07
sadness	0.16	0.07	0.07	-0.01	0.13	0.07
trustworthiness	-0.62	-0.28	-0.05	-0.23	0.31	0.16
dominance	0.05	0.16	0.12	-0.13	-0.02	0.04
hue	0.27	0.20	0.19	0.03	0.01	-0.08
eye gaze	0.13	0.28	-0.10	0.13	-0.29	-0.04
age	-0.09	0.14	0.12	-0.09	0.67	0.40
anger	0.00	0.00	0.00	0.00	0.00	0.00
fear	0.19	0.12	0.08	-0.07	0.04	0.00
surprise	0.07	0.12	0.03	-0.07	-0.06	0.13

**Learning Architecture.** The network  $\phi$  contains a single linear layer with no bias which takes a constant (1) as an input and outputs a number  $z_i$  for each data dimension  $i$ .

The network  $\hat{h}$  takes as input  $(x, w, y)$ . It contains one linear layer with no bias which takes as input  $[x, y]$  and outputs a single number  $\hat{s}$ . The second linear layer (with bias) takes as input  $w$  and outputs the sigmoid activation of a single number,  $switch$ , representing the propensity to incorporate  $s$  at  $w$ . It then outputs  $w^\top x + switch \cdot \hat{s}$ .

#### Baselines.

- **Machine Only:** The best possible linear model (with bias) trained to predict  $y$  from  $x_1 \dots x_4$ .
- **$h(\text{Machine})$ :** The human model  $h$  applied to the best possible linear model (with bias) trained to predict  $y$  from  $x_1 \dots x_4$ .

$$h(\text{Machine}) = \beta_0 + h(x, \beta_1, \dots, \beta_4, s)$$

where  $\beta$  are the coefficients selected by the machine-only regression.

#### Human Models

- **Always:** The human always fully incorporates the side information,

$$h(x, w, s) = w^\top x + s$$

- **Never:** The human never incorporates the side information,

$$h(x, w, s) = w^\top x$$

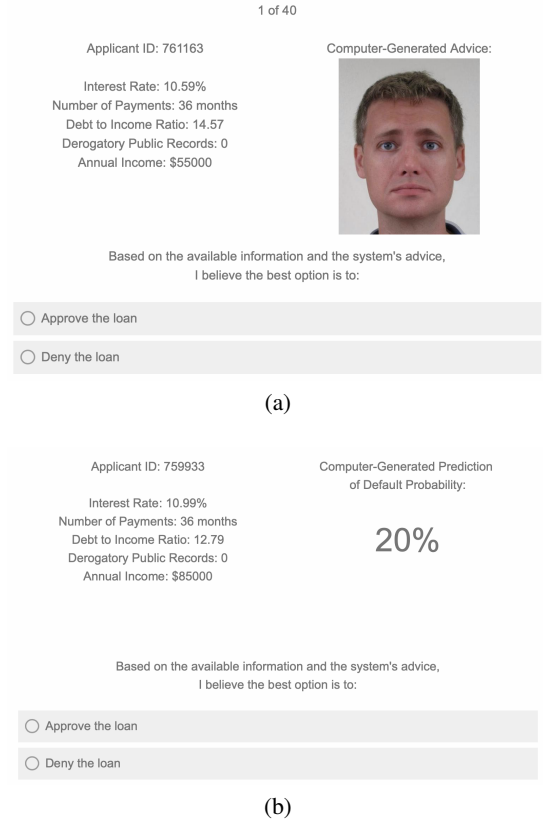


Figure 9: Images from mTurk questionnaire

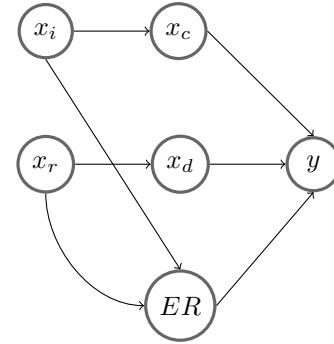


Figure 10: Relationship of variable correlations in the side information experiment

- **Or:** The human becomes less likely to incorporate side information as weight is put on  $x_i, x_r$ ,

$$h(x, w, s) = w^\top x + \sigma(1/\max(\max(x_i, x_r), .0001) - 2) \cdot s$$

Note that  $\max(.0001)$  is required to prevent numerical overflow, and  $-2$  recenters the sigmoid to allow for values  $< .5$ .

- **Coarse:** The human incorporates  $s$  as in Or, but uses a coarse, noisy version of  $s$ ,  $s' = 2 \cdot \mathbb{1}\{s \geq .5\}$

$$h(x, w, s) = w^\top x + \sigma(1/\max(\max(x_i, x_r), .0001) - 2) \cdot s'$$



## **Appendix D   Select Turker quotes**

- “I wasn’t always looking at just happiness or sadness. Sometimes the expressions seemed disingenuously happy, and that also threw me off. I don’t know if that was intentional but it definitely effected my gut feeling and how I chose.”
- “In my opinion, the level of happiness or sadness, the degree of a smile or a frown, was used to represent applications who were likely to be payed back. The more happy one looks, the better the chances of the client paying the loan off (or at least what the survey information lead me to believe).”
- “I was more comfortable with facial expressions than numbers. I felt like a computer and I didn’t feel human anymore. Didn’t like it at all.”

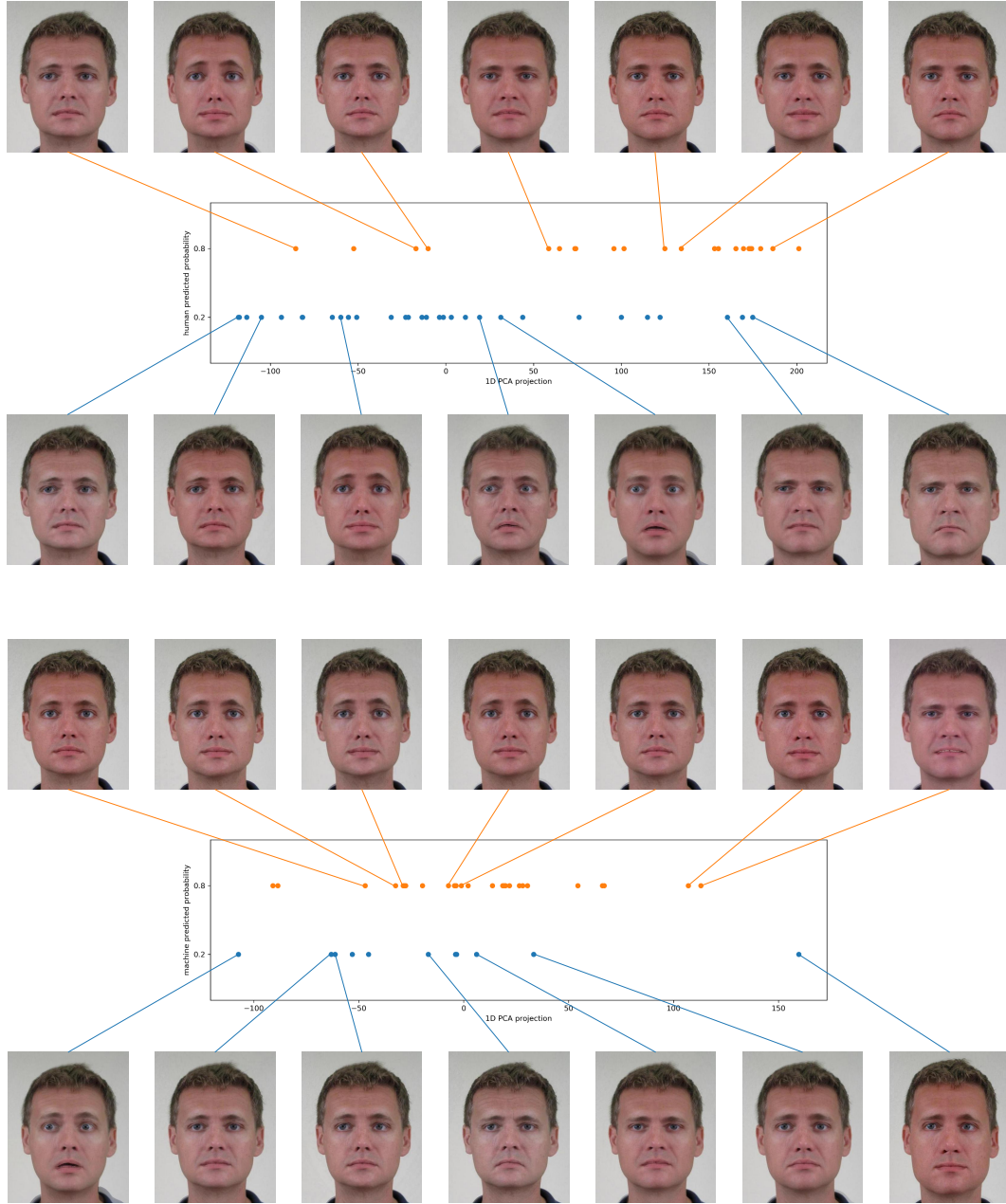


Figure 8: Richness of avatar representation. A visualization of 200 avatars randomly sampled from the held-out test set, grouped by either human (top) or machine (bottom) predictive probability (0.2 in blue, 0.8 in orange, with a tolerance of 0.05). Avatars are positioned based on a 1D PCA dimensionality reduction of their corresponding feature vectors  $z$ , along which a ‘gradient’ of facial changes can be observed. **Top:** Here avatars are grouped by human predictive probability. The figure shows how for the same human decisions, learning results in avatars of varied and complex facial expressions, conveying rich high-dimensional information. Interestingly, avatars corresponding to loan denial exhibit more variance, suggesting that there may be more ‘reasons’ for denying a loan than for approving one. **Bottom:** Here avatars are grouped by machine predictive probability. Since all examples in each group have the same predictive probability, they are equally similar, which does not facilitate a clear notion for reasoning. In contrast, avatars maintain richness in variation, and can be efficiently used for reasoning (e.g., via similarity arguments) and other downstream tasks.